Published in final edited form as:
Mol Microbiol. 2011 November ; 82(4): 836–850. doi:10.1111/j.1365-2958.2011.07831.x.

RbsB (NTHI_0632) mediates quorum signal uptake in nontypeable *Haemophilus influenzae* strain 86-028NP

Chelsie E. Armbruster, **Bing Pang**, **Kyle Murrah**, **Richard A. Juneau**, **Antonia C. Perez**, **Kristin E.D. Weimer**, and **W. Edward Swords***
Department of Microbiology and Immunology, Wake Forest University Health Sciences, Winston Salem, NC 27157, United States of America

Summary

Nontypeable *Haemophilus influenzae* (NTHI) is a respiratory commensal and opportunistic pathogen, which persists within biofilms on airway mucosal surfaces. For many species, biofilm formation is impacted by quorum signaling. Our prior work shows that production of autoinducer-2 (AI-2) promotes biofilm development and persistence for NTHI 86-028NP. NTHI 86-028NP encodes an ABC transporter annotated as a ribose transport system that includes a protein (RbsB) with similarity to the *Escherichia coli* LsrB and *Aggregatibacter actinomycetemcomitans* RbsB proteins that bind AI-2. In this study, inactivation of *rbsB* significantly reduced uptake of AI-2 and the AI-2 precursor dihydroxypentanedione (DPD) by NTHI 86-028NP. Moreover, DPD uptake was not competitively inhibited by ribose or other pentose sugars. Transcript levels of *rbsB* increased in response to DPD and as bacteria approached stationary-phase growth. The NTHI 86-028NP *rbsB* mutant also formed biofilms with significantly reduced thickness and total biomass and reduced surface phosphorylcholine, similar to a *luxS* mutant. Infection studies revealed that loss of *rbsB* impaired bacterial persistence in the chinchilla middle-ear, similar to our previous results with *luxS* mutants. Based on these data, we conclude that in NTHI 86-028NP, RbsB is a LuxS/AI-2 regulated protein that is required for uptake of and response to AI-2.

Keywords

Nontypeable *Haemophilus influenzae*; autoinducer-2; biofilm; otitis media

Introduction

Nontypeable *Haemophilus influenzae* (NTHI) inhabits the nasopharynx and upper airways of children and healthy adults (Erwin & Smith, 2007, Faden *et al.*, 1991), and can cause opportunistic infections of the airway mucosa that include bronchitis, sinusitis, and otitis media (OM) (Erwin & Smith, 2007, Pichichero, 2000). Among these infections, OM is of particular public health importance. For example, OM is an extremely pediatric infection, affecting the majority of all children (Klein, 2000, Mandel *et al.*, 2008), and is a leading cause for pediatric office visits and new antibiotic prescription to children (Finkelstein *et al.*, 2001).

OM infections are often chronic and/or recurrent in nature, and can be highly resistant to immune clearance and antibiotic treatment. Thus, it is generally thought that OM involves persistence of bacteria within biofilm communities (Costerton *et al.*, 1999, Bakaletz, 2007,

*Corresponding author Mailing address: 5053 Hanes Biomedical Research Building, Medical Center Boulevard, Winston-Salem, NC 27157, Phone: (336) 713-5049, Fax: (336) 716-9928, wswords@wfubmc.edu.

Post *et al.*, 2007). Bacterial biofilms have been observed directly in patient samples (Hall-Stoodley *et al.*, 2006, Hoa *et al.*, 2009, Nistico *et al.*, 2011, Post, 2001) and in the chinchilla experimental model for OM (Ehrlich *et al.*, 2002, Post, 2001). As biofilms provide protection from the immune response and antibiotic treatment, understanding the mechanisms involved in their formation during chronic infection may provide new targets for disruption and treatment of biofilm-related infections (Armbruster & Swords, 2010).

Biofilm formation for many bacterial species is controlled in part through cell density-dependent quorum signaling networks, wherein changes in bacterial population phenotypes are mediated by accumulation of a soluble signaling mediator (Hardie & Heurlier, 2008, Jayaraman & Wood, 2008, Miller & Bassler, 2001, Waters & Bassler, 2005). Such signaling networks include autoinducer-2 (AI-2), a ribose derivative produced by both Gram-negative and Gram-positive bacteria that is conserved among numerous bacterial species and thus referred to as an inter-species signal (Jayaraman & Wood, 2008, Waters & Bassler, 2005). Mutation of the genetic determinant of AI-2 production (*luxS*) was previously shown to impact biofilm thickness/maturation and persistence of NTHI strain 86-028NP in an experimental animal model of OM (Armbruster *et al.*, 2009). The focus of this study is to understand how strain NTHI 86-028NP internalizes and responds to AI-2.

In *Vibrio harveyi*, sensing of AI-2 occurs through a two-component system involving LuxP and LuxQ (Bassler *et al.*, 1994). LuxP is similar to periplasmic ribose binding proteins and binds AI-2, while LuxQ contains sensor kinase and response regulator domains to propagate the signal (Henke & Bassler, 2004). *Salmonella typhimurium, Escherichia coli*, *Sinorhizobium meliloti*, and *Aggregatibacter actinomycetemcomitans* utilize the Lsr (LuxS regulated) ABC transporter, an AI-2 transport system similar to the ribose ABC transporter (Miller *et al.*, 2004). Rather than the two-component signal cascade described in *V. harveyi*, the Lsr system mediates AI-2 uptake via binding by LsrB and transport through a heterodimeric membrane channel (Pereira *et al.*, 2008, Michiko E. Taga, 2001, Xavier & Bassler, 2005, Shao *et al.*, 2007b). In addition to LsrB, it was determined in *A. actinomycetemcomitans* that the ribose binding protein RbsB also interacts with AI-2 (Shao *et al.*, 2007a, James *et al.*, 2006).

NTHI 86-028NP does not possess a homolog of LuxPQ transport system. However, the NTHI 86-028NP genome contains an ABC transporter annotated as a ribose transport system that includes a binding protein encoded by NTHI_0632, designated *rbsB* (Harrison *et al.*, 2005). The NTHI 86-028NP *rbsB* gene product has 40.3 percent identity to *E. coli* LsrB, and 87 percent identity to *A. actinomycetemcomitans* RbsB that was found to bind AI-2. The predicted RbsB proteins from *H. influenzae* 86-028 NP and *A. actinomycetemcomitans* are virtually identical in length (292 vs. 293 amino acids). LsrB from *A. actinomycetemcomitans* is predicted to be somewhat larger (365 amino acids). Based on these observation and the similarity between the Lsr AI-2 transport system and ribose transporters, it was hypothesized that NTHI 86-028NP may utilize RbsB for internalization of and response to AI-2. An *rbsB* mutant was therefore generated in NTHI 86-028NP to determine the impact of this mutation on production and internalization of AI-2, biofilm formation, and the ability of NTHI to establish a chronic infection in the chinchilla model of OM.

Results

Construction and confirmation of NTHI 86-028NP rbsB::Cm

A null allele of *rbsB* (NTHI_0632) was constructed by insertion of a chloramphenicol resistance cassette into the coding sequence (see Experimental Procedures). This allele was introduced into NTHI 86-028NP by natural transformation and verified by PCR (data not

shown). No differences in growth rate were observed for NTHI 86-028NP *rbsB*::Cm compared to the parental strain in rich broth culture. NTHI 86-028NP and NTHI 86-028NP *rbsB*::Cm also grew similarly in minimal media with glucose as a carbon source, and neither strain was able to utilize ribose as a sole carbon source (data not shown). Notably, supernatant samples taken during growth in rich media and assessed for AI-2 using the *Vibrio harveyi* bioluminescence assay revealed a significant accumulation of AI-2 in NTHI 86-028NP *rbsB*::Cm supernatants during late-exponential and early-stationary phase (Figure 1). In contrast, the level of AI-2 in supernatant harvested from cultures of the parental strain decreased at these time points, suggesting that strain NTHI 86-028NP begins to internalize AI-2 in an *rbsB*-dependent manner as it approaches stationary phase. Importantly, genetic complementation of NTHI 86-028NP *rbsB*::Cm via insertion of the wild type *rbsB* allele into an intergenic region of the chromosome (*IRB*, see Experimental Procedures) restored the ability of this strain to decrease AI-2 levels in stationary phase.

RbsB mediates AI-2 uptake in NTHI 86-028NP

To further investigate the role of *rbsB* in depletion or internalization of AI-2, NTHI 86-028NP *luxS*::Kn was utilized to study the kinetics of AI-2 depletion during growth, independent of AI-2 production. Broth cultures were inoculated with NTHI 86-028NP *luxS*::Kn and supplemented with the synthetic AI-2 precursor (S)-4,5-Dihydroxy-2,3-pentanedione (DPD) as indicated, and samples were taken to assess the amount of DPD remaining in the cultures over time (Figure 2A). By the time the cultures reached stationary phase, NTHI 86-028NP *luxS*::Kn had depleted the majority of DPD present in the culture. In contrast, only a minimal loss of DPD was observed in an uninoculated control. As expected, NTHI 86-028NP *luxS*::Kn did not produce detectable AI-2 at any point during the course of growth. Notably, mutation of *rbsB* in an NTHI 86-028NP *luxS*::Kn background almost completely abrogated depletion of DPD by this strain (Figure 2A). In five replicate experiments, NTHI 86-028NP *luxS*::Kn depleted 60% of DPD from culture supernatants on average by the time the cultures reached an OD_{600} of approximately 0.85, while the double mutant only depleted 15% of total DPD signal (Figure 2B). In addition, DPD levels were unaffected by cell-free culture supernatants from NTHI 86-028NP *luxS*::Kn and NTHI 86-028NP *rbsB*::Cm *luxS*::Kn, indicating that DPD is not being degraded by factors present in the culture supernatants (data not shown).

Because *rbsB* is designated as the binding protein for a ribose transport system, we next tested the impact of ribose on DPD uptake. NTHI 86-028NP *luxS*::Kn was cultured in media supplemented with 0.2 μM DPD alone or with increasing concentrations of ribose, and samples were taken when the cultures reached an OD_{600} of approximately 0.85 for assessment of DPD depletion (Table 1). The addition of 0.1 mM ribose had no effect on DPD depletion, while ribose in excess of 1 mM inhibited depletion of DPD. Notably, this inhibition of depletion only occurred when ribose was present in 5000-fold molar excess, suggesting a higher affinity for AI-2 than for ribose. Incubation with millimolar concentrations of another pentose sugar (xylose) also limited DPD depletion, while the addition of sucrose had no impact (Table 1). Based on these results, we conclude that in NTHI strain 86-028NP, *rbsB* is part of an AI-2 transport system with lower affinity for pentose sugars.

RbsB transcript levels correlate with AI-2 production

For some bacterial species, expression of the AI-2 transport system is induced by the presence of AI-2 (Taga *et al.*, 2001). It was therefore hypothesized that if the protein encoded by *rbsB* functions as an AI-2 binding protein, transcript levels may increase during late-exponential phase when bacteria reach peak AI-2 production. NTHI 86-028NP and NTHI 86-028NP *luxS*::Kn were therefore cultured in rich media to stationary phase, and

samples were taken at various time points during growth to assess transcript levels for *luxS* and *rbsB* by real time RT-PCR (Figure 3). For NTHI 86-028NP, *luxS* transcript levels increased by approximately two-fold during late-exponential phase (Figure 3A), and *rbsB* transcript levels increased by approximately five-fold during late-exponential to early-stationary phase (Figure 3B). Notably, both *luxS* and *rbsB* transcript levels remained low in the *luxS* mutant (Figure 3A and 3B). As NTHI 86-028NP *luxS*::Kn was shown to deplete AI-2 from culture in Figure 2, low level expression of *rbsB* must still be sufficient to mediate AI-2 uptake, whereas increased expression of *rbsB* may be optimal for internalization of the high concentration of AI-2 encountered during early-stationary phase. Additionally, incubation of the *luxS* mutant with DPD resulted in a transient 8-fold increase in *rbsB* transcript levels compared to a control culture (Figure 3C), indicating that *rbsB* transcription increases in response to AI-2 signaling. From these data, we conclude that transcription of *rbsB*, and *luxS* to a lesser extent, are regulated by AI-2 signaling.

Both rbsB and luxS promote biofilm maturation

Previous studies with the NTHI 86-028NP *luxS* mutant showed that loss of AI-2 quorum signaling altered overall biofilm development and maturation, resulting in biofilms with reduced biomass and average thickness (Armbruster et al., 2009). As *rbsB* is necessary for depletion of DPD, we hypothesized that mutation of *rbsB*, and the concomitant loss of AI-2 internalization would diminish biofilm maturation, as we have previously observed for *luxS* mutants. To test this hypothesis, NTHI 86-028NP, NTHI 86-028NP *luxS*::Kn, and NTHI 86-028NP *rbsB*::Cm were cultured in a continuous flow system to establish biofilms. Both mutants formed visible biofilms in the continuous flow system. Biofilms visualized by Live/Dead staining revealed differences in biofilm thickness by confocal laser scanning microscopy (CLSM) for NTHI 86-028NP *luxS*::Kn and NTHI 86-028NP *rbsB*::Cm compared to the parental strain (Figure 4). Representative three-dimensional images of biofilms formed by each strain demonstrate the reduced biofilm biomass for the quorum signaling mutants (Figure 4A-C). Similar to our previous work with NTHI 86-028NP *luxS*::Kn, both the *luxS* mutant and 86-028NP *rbsB*::Cm formed biofilms with significantly decreased biomass (Figure 4D), surface to biovolume ratio (Figure 4E), average thickness (Figure 4F), and maximum thickness (Figure 4G) compared to the parental strain.

Stationary biofilms were also established by NTHI 86-028NP, NTHI 86-028NP *luxS*::Kn, NTHI 86-028NP *rbsB*::Cm, and the complemented strain NTHI 86-028NP *rbsB*::Cm *IRB*::Sp to verify the results obtained under continuous media flow conditions and to determine the impact of genetic complementation on biofilm formation by the *rbsB* mutant (Figure 5). Live/Dead staining and CLSM of biofilms formed by each strain demonstrated that NTHI 86-028NP *luxS*::Kn (Figure 5D) and NTHI 86-028NP *rbsB*::Cm (Figure 5C) also formed thinner biofilms with reduced total biomass (Figure 5E) and average thickness (Figure 5F) as compared to the parental strain NTHI 86-028NP (Figure 5A) when cultured under stationary conditions. Notably, genetic complementation of *rbsB* fully restored biofilm formation by this strain as the biofilms formed by NTHI 86-028NP *rbsB*::Cm *IRB*::Sp were similar to those formed by the parental strain (Figure 5B, 5E, 5F). From these studies, we conclude that mutation of *rbsB* and the resulting loss of AI-2 internalization impacts biofilm formation in a similar manner as loss of AI-2 production.

To further investigate the impact of AI-2 quorum signaling on biofilm formation, NTHI 86-028NP, NTHI 86-028NP *luxS*::Kn, and NTHI 86-028NP *rbsB*::Cm stationary biofilms were formed in the presence or absence of DPD, and biofilms were analyzed for changes in total biomass (Figure 6). In media lacking DPD, NTHI 86-028NP formed thick biofilms while NTHI 86-028NP *luxS*::Kn and NTHI 86-028NP *rbsB*::Cm biofilms had significantly decreased total biomass (Figure 6A) and average thickness (Figure 6B), as previously observed. The addition of 0.2 μM DPD to NTHI 86-028NP did not significantly alter

biofilm formation. For NTHI 86-028NP *luxS*::Kn, the addition of DPD fully restored biofilm biomass and thickness to the level observed for the parental strain. Notably, NTHI 86-028NP *rbsB*::Cm did not respond to DPD, as indicated by low biofilm biomass and average thickness under both treatment conditions. Taken together, these results provide concrete evidence that the biofilm defects observed for NTHI 86-028NP *luxS*::Kn are the direct result of loss of AI-2 signaling rather than a metabolic defect due to mutation of *luxS*, and that *rbsB* is required by NTHI strain 86-028NP to respond to AI-2.

The decreased biofilm thickness and total biomass observed for NTHI 86-028NP *luxS*::Kn were previously attributed in part to alterations in lipooligosaccharide (LOS) moieties (Armbruster et al., 2009). Specifically, NTHI 86-028NP *luxS*::Kn had decreased phosphorylcholine (*P*Cho), an LOS modification that correlates with biofilm maturation and persistence in vivo (Hong et al., 2007a, Hong et al., 2007b). The level of surface-accessible *P*Cho on NTHI 86-028NP *rbsB*::Cm was assessed by whole-bacterium ELISA for comparison to NTHI 86-028NP, NTHI 86-028NP *luxS*::Kn, and NTHI 86-028NP *licD*::Kn, a mutant lacking the *P*Cho transferase that is thus unable to decorate LOS with *P*Cho (Figure 7). As previously reported, NTHI 86-028NP *luxS*::Kn had significantly reduced surface-accessible *P*Cho compared to the parental strain. NTHI 86-028NP *rbsB*::Cm also had reduced *P*Cho as compared to the parental strain. Notably, the amount of surface-accessible *P*Cho detected on NTHI 86-028NP *rbsB*::Cm was almost identical to the level detected on NTHI 86-028NP *luxS*::Kn. NTHI 86-028NP *licD*::Kn had negligible surface-accessible *P*Cho, as expected.

The biosynthetic genes involved in *P*Cho decoration of LOS, as well as other LOS moieties, are subject to phase variation via slip-strand mispairing within repeat regions (Weiser, 2000). Therefore, the phase status of seven LOS biosynthetic genes was assessed for NTHI 86-028NP *rbsB*::Cm for comparison to the parental strain (see Experimental Procedures). No differences were observed for the phase status of genes involved in *P*Cho decoration of LOS (Table 2). Additionally, NTHI 86-028NP *rbsB*::Cm phase status only differed from that of NTHI 86-028NP for *oafA*, which was generally in the “ON” phase for NTHI 86-028NP *rbsB*::Cm colonies and in the “OFF” phase within most NTHI 86-028NP colonies. Interestingly, altered phase status of *oafA* was also observed for NTHI 86-028NP *luxS*::Kn (Armbruster et al., 2009). The results of the phase status assessment clearly show that the reduction in surface-accessible *P*Cho observed for NTHI 86-028NP *rbsB*::Cm was not due to phase variation of the LOS biosynthetic genes necessary for the addition of *P*Cho to LOS.

Both rbsB and luxS promote the establishment of chronic NTHI infection

Our previous study of NTHI 86-028NP *luxS*::Kn showed that production of AI-2 was a critical factor in the ability of nontypeable *H. influenzae* to establish a persistent infection in the chinchilla model of otitis media (Armbruster et al., 2009). Based on the similarities between NTHI 86-028NP *luxS*::Kn and NTHI 86-028NP *rbsB*::Cm biofilm formation and *P*Cho expression, it was hypothesized that mutation of *rbsB* and the resulting defect in AI-2 internalization would result in a similar persistence defect in the chinchilla model of otitis media. To test this hypothesis, chinchillas were inoculated via transbullar injection of approximately 10^3 cfu/ear of NTHI 86-028NP, NTHI 86-028NP *luxS*::Kn, or NTHI 86-028NP *rbsB*::Cm, and bacterial load was determined at 7, 14, 21, and 28 days post-infection. Comparable numbers of each strain were recovered at 7 and 14 days post-infection (Figure 8). By 21 days post-infection, a significant persistence defect was observed for the quorum signaling mutants with 13% of ears (2 of 16) infected with NTHI 86-028NP *luxS*::Kn and 31% of ears (5 of 16) infected with NTHI 86-028NP *rbsB*::Cm clear of visible signs of infection and with bacterial loads below the limit of detection. A similar trend was observed at 28 days post-infection, with bacterial loads below the limit of detection

observed in 33% ears (2 of 6) infected with NTHI 86-028NP *luxS*::Kn and 50% of ears (4 of 8) infected with NTHI 86-028NP *rbsB*::Cm. Notably, for animals infected with the parental strain NTHI 86-028NP a bacterial load greater than the initial inocula of 10^3 cfu/ear was detected at all times post-infection. We thus conclude that *rbsB* encodes a protein critical for AI-2 quorum signaling in NTHI strain 86-028NP, that the AI-2 signaling system promotes the establishment of biofilms in vitro, and that AI-2 signaling also promotes the establishment of chronic infection by NTHI.

Discussion

It has long been recognized that bacteria can persist within biofilm communities during chronic disease, and establishment of these bacterial communities affords protection from both immune clearance and antibiotic treatment (Anderson & O'Toole, 2008, Stewart, 2002, Ghannoum & O'Toole, 2004, Costerton *et al.*, 2003). Due to the high rate of antibiotic resistance for chronic biofilm diseases such as OM, research focused on identifying factors which contribute to the establishment of bacterial biofilms and persistence will further our understanding of biofilm-associated disease and may aid in the development of new therapeutics. One factor which contributes to biofilm formation, maturation, and dispersal for many species is bacterial cell-to-cell communication via quorum signals (Davies *et al.*, 1998, Hardie & Heurlier, 2008). Our previous work established that NTHI 86-028NP produces AI-2 and requires *luxS* to form mature biofilms and establish a chronic infection (Armbruster et al., 2009), but it was unclear as to how strain 86-028NP was responding to this signaling mediator. In this study, we used a genetic approach to identify *rbsB* as being required for uptake of and response to AI-2 by NTHI 86-028NP, and further addressed the role of AI-2 quorum signaling in biofilm development and persistence. The results of this study clearly show that sensing of AI-2 promotes the establishment of mature NTHI biofilm communities in vitro and during experimental OM.

While previous work from our laboratory reported a prominent role for *luxS* in biofilm maturation and persistence, the product of *luxS* is a component of the activated methyl cycle and therefore plays a role in bacterial metabolism. Thus, for some species, the effects of a *luxS* mutation on biofilm development and virulence can be attributed to a metabolic defect rather than interference with production and sensing of AI-2 (Rezzonico & Duffy, 2008, Sztajer *et al.*, 2008, Winzer *et al.*, 2002, Winzer *et al.*, 2003). However, through the use of the AI-2 precursor DPD in the present study, we have clearly shown that the biofilm defects of a *luxS* mutant can be fully complemented by the addition of quorum signal. The results of this study also prove that mutation of a gene involved in the response to AI-2 in a strain with *luxS* intact still results in defects in biofilm maturation, indicating that this phenotype in NTHI 86-028NP is due to loss of AI-2 quorum signaling rather than any potential metabolic impact of the *luxS* mutation. Both the *luxS* mutant and the *rbsB* mutant exhibited decreased phosphorylcholine levels, indicating that AI-2 signaling regulates the formation of mature NTHI biofilms at least in part through modulation of LOS composition (Armbruster et al., 2009). Additionally, the results of the phase status analyses in concert with our previous study of the *luxS* mutant clearly exclude the possibility of an unlinked phase variation event resulting in the observed changes in biofilm maturation.

In *E. coli,* the LuxS-regulated (Lsr) operon for internalization of AI-2 includes *lsrA, lsrC, lsrD, lsrB,* the genes *lsrF, lsrG,* and *lsrE* that appear to be involved in degradation of AI-2, and a divergently transcribed gene cluster containing *lsrK* and the repressor *lsrR* (Li et al., 2007, Taga et al., 2003, Wang et al., 2005, Xavier & Bassler, 2005). In contrast, the ribose transport operon of NTHI 86-028NP which includes *rbsB* is composed of *rbsD, rbsA, rbsC, rbsB, rbsK,* and *rbsR* (Harrison et al., 2005). This configuration is more similar to the σ-ribose transport operon of *Aggregatibacter actinomycetemcomitans* HK1651

(www.oralgen.lanl.gov) than to the Lsr transport operon. Additionally, *rbsK* and *rbsR* do not appear to be divergently transcribed in NTHI, and the genes involved in degradation of AI-2 are lacking. However, as NTHI 86-028NP lacks a true Lsr transporter, this strain appears to be utilizing the putative ribose transporter as an AI-2/LuxS-regulated transporter for uptake of and response to AI-2. In support of this hypothesis, transcription of the *lsr* operon in *S. typhimurium* and *E. coli* is regulated by AI-2 and thus decreased in a *luxS* mutant (Taga et al., 2001, Xavier & Bassler, 2005). Therefore, the data reported herein showing low *rbsB* transcript levels in NTHI 86-028NP *luxS*::Kn and upregulation of transcript levels following the addition of DPD prove that *rbsB* is regulated by LuxS and AI-2 in NTHI 86-028NP.

Based on these results, *rbsB* in NTHI 86-028NP clearly represents an AI-2-regulated and *luxS*-regulated (Lsr) gene even though the operon containing *rbsB* is more similar to the ribose transport operon of *A. actinomycetemcomitans* than the Lsr operon of *E. coli*. In addition, the minimal impact of pentose sugars on depletion of DPD (unless in excess of 5000 times the DPD concentration) supports the conclusion that, for NTHI strain 86-028NP, *rbsB* is utilized as an AI-2 transporter at high cell density. It is therefore intriguing to speculate that the rest of the ribose transport operon of NTHI 86-028NP may be similarly regulated by AI-2 and function as part of a high-affinity AI-2 transporter, in addition to its possible function as a pentose sugar transporter. However, further research will be necessary to determine how the operon is regulated without apparent divergent transcription of the operon repressor. The downstream phosphorylation and detection of AI-2 and the signaling induced in response to detection of AI-2 also remain to be investigated in NTHI.

In the context of experimental OM, both the *luxS* mutant and the *rbsB* mutant were below the limit of detection in 13% to 50% of samples taken at 21 days post-infection or later while NTHI 86-028NP continued to persist at high levels in all animals infected with this strain. Based on these data quorum signaling does not appear to be required for acute infection, but the ability to both produce and respond to the AI-2 signal clearly contribute to the establishment of a chronic infection. This defect in persistence during chronic infection may be related to the biofilm defects observed for the quorum signaling mutants, in that minimal biofilm formation by the mutant strains may be sufficient to promote persistence during acute infection, but the formation of mature phosphorylcholine-positive biofilm communities may be necessary for the establishment and maintenance of a chronic infection and evasion of the host immune response.

In addition, while a clear trend towards clearance was observed for the quorum signaling mutants it is notable that the animals which still had detectable levels of the mutant strains at later time points carried a similar bacterial load as that observed for animals infected with the parental strain. As these infection studies are conducted using an outbred population, this difference between apparent clearance and persistence may reflect heterogeneity in the immune responses of individual chinchillas and their ability to combat the infection. However, as all 52 ears infected with the parental strain exhibited a bacterial load higher than the initial inocula regardless of the number of days post-infection, these results suggest that the quorum signaling mutants are most likely more susceptible to factors of the host immune response than the parental strain. The results of the infection studies thus suggest that either only some of the animals were able to mount a sufficient immune response to promote clearance of the mutant strains, or that the quorum signaling mutants managed to overcome the defect in AI-2 signaling and/or biofilm maturation to establish a persistent population in some of the infected ears. Further research will be necessary to distinguish between these possibilities.

Similar to the results of the in vitro biofilm studies, the results of experimental infection with the *luxS* mutant and the *rbsB* mutant prove that the persistence defect previously

observed for NTHI 86-028NP *luxS*::Kn was due to loss of AI-2 quorum signaling rather than any potential metabolic defects or to alterations in other quorum signaling networks, such as AI-3, which may be impacted by a *luxS* mutation (Kendall *et al.*, 2007). However, it still remains a possiability that host factors produced during the course of infection could impact NTHI signaling networks and contribute to biofilm formation and persistence. The data presented herein thus support a prominent role for AI-2 quorum signaling in concert with other as yet undetermined factors that promote the establishment of a chronic, biofilm-associated infection. It is also possible that a mutant deficient in both the ability to produce and respond to AI-2 may have a more severe persistence defect beyond what was observed for either quorum signaling mutant strain.

NTHI remains a leading cause of OM and other upper respiratory tract infections, despite promising vaccine candidates. Our data indicate that AI-2 quorum signaling is utilized by strain 86-028NP to promote biofilm formation and establishment of chronic, persistent infections. Furthermore, our previous work indicates that AI-2 produced by NTHI impacts *Moraxella catarrhalis* biofilm formation, antibiotic resistance, and persistence in the chinchilla model of OM (Armbruster *et al.*, 2010, Verhaegh *et al.*). Therefore, therapeutics aimed at interfering with AI-2 binding and signaling may prevent biofilm development or disrupt already established biofilms to augment current OM treatments. For NTHI 86-028NP, *rbsB* appears to be a promising target for interference with AI-2 signaling as mutation of this gene clearly has a significant biological impact on AI-2 uptake, biofilm development, and persistence during experimental OM. However, it should be noted that there is considerable genomic heterogeneity among NTHI strains and that some NTHI strains possess both the ribose transport operon and an Lsr transport operon, similar to *A. actinomycetemcomitans*. Thus, it is possible that other NTHI strains may utilize different means for uptake of quorum signal, or that other strains may respond to AI-2 signaling in a different manner. Further investigation into transport and sensing of AI-2 in NTHI will allow for identification of virulence factors controlled by AI-2 signaling, and may reveal new target candidates for disruption of quorum signaling as a therapy for treatment of NTHI infections.

Experimental Procedures

Bacterial strains and culture conditions

All strains of nontypeable *H. influenzae* were cultivated in brain heart infusion (BHI) medium (Difco) supplemented with 10 μg/mL hemin (ICN Biochemicals) and 10 μg/mL NAD (Sigma); this medium is referred to below as supplemented BHI (sBHI). Nontypeable *H. influenzae* (NTHI) strain 86-028NP is a nasopharyngeal isolate from a child with chronic otitis media (Bakaletz *et al.*, 1988) for which the genomic sequence has been determined (Harrison et al., 2005). NTHI 86-028NP *luxS*::Kn contains a kanamycin resistance cassette disrupting the autoinducer-2 synthase (NTHI_0621) (Armbruster et al., 2009). NTHI 86-028NP *licD*::Kn contains a kanamycin resistance cassette disrupting the phosphorylcholine transferase (NTHI_1594) (West-Barnette *et al.*, 2006).

Generation of NTHI 86-028NP rbsB::Cm

A 2313 bp DNA fragment containing *rbsB* (NTHI_0632) was amplified from NTHI 86-028NP genomic DNA using primers GCA ATC GCC GCT TCA ATG G and CTA CCG CTA CCC CCG TCA GG. The amplicon was ligated into pCR2.1 following InVitrogen protocol to generate pCR-*rbsB*. pCR-*rbsB* was digested with *Ssp*I, a unique site within *rbsB*, for ligation with a chloramphenicol resistance cassette from pCMR (Whitby *et al.*, 1998). The resulting construct was transformed into chemically-competent *E. coli* to generate pCR-*rbsB*::Cm. The expected sequence was confirmed by PCR with primers GGT TTG GCT

GTT TCT GGC TCT GC and CGA TAG TTG CTG CCA TTT TGC CAC, and by sequence analysis. The plasmid DNA was linearized with *Bam*HI and introduced into NTHI 86-028NP via natural transformation as described previously (Hong et al., 2007a, Hong et al., 2007b). Transformants were plated onto sBHI agar containing 1.5 μg/ml chloramphenicol (Sigma) and incubated for 48 h at 37 °C. Transformants carrying the expected construct were verified by PCR.

Generation of NTHI 86-028NP rbsB::Cm IRB::rbsB

A 1363 bp intergenic region (herein designated as intergenic region B, or *IRB*) is contained within the NTHI 86-028NP genome between NTHI_1846 and NTHI_1849. A 2248 bp segment containing *IRB* was amplified from NTHI 86-028NP genomic DNA using primers AGC TTC CGC CGC CAG TAA AAT and CCA AAG CGT CAG CGG ATG C. The amplicon was ligated in pCR2.1 using the TA Cloning Kit (InVitrogen) to create pCR-*IRB*. White colonies were verified to contain *IRB* using primers CCG CGT CCG AAA TAT GTG CTA C and ACT CCG CGT TAT CCC CGT CTT A. pCR-*IRB* was digested with *Ssp*I and dephosphorylated. A spectinomycin resistance cassette was excised from pSpec (Whitby et al., 1998) with *Eco*RV and ligated into the prepared pCR-*IRB* vector. The resulting construct was transformed into chemically-competent *E. coli* to generate pCR-*IRB*::Sp. pCR-*IRB*::Sp was digested with *Stu*I and dephosphorylated. pCR-*rbsB* (described above) was digested with *Btg*I and *Bsm*FI, and the 1134 bp band containing *rbsB* was gel extracted and ligated into pCR-*IRB*::Sp. The resulting construct was transformed into chemically-competent *E. coli* to generate pCR-*IRB::rbsB*. Transformants were selected by growth on LB plates with 100 μg/ml spectinomycin (Sigma), screened using primers M13F (a universal primer in pCR2.1) and CAC GGT ACC ATT TCT TGC TG (within the spectinomycin resistance cassette), and verified by restriction digest with *Nde*I and *Eco*RV to generate three bands (4118 bp, 3435 bp, and 938 bp). pCR-*IRB::rbsB* was linearized using *Bam*HI and introduced into NTHI 86-028NP *rbsB*::Cm via natural transformation. Transformants were plated onto sBHI agar containing 30 μg/ml spectinomycin, and verified by PCR to contain both *rbsB* and *rbsB*::Cm using primers GGT TTG GCT GTT TCT GGC TCT GC and CGA TAG TTG CTG CCA TTT TGC CAC.

Generation of NTHI 86-028NP rbsB::Cm luxS::Kn

A double mutant strain was generated by disruption of *luxS* (NTHI _0621) in NTHI 86-028NP *rbsB*::Cm. The previously published plasmid pUC*luxS*::Kn (Armbruster et al., 2009) was linearized with *Sfo*I and introduced into NTHI 86-028NP *rbsB*::Cm via natural transformation. Transformants were plated onto sBHI agar containing 30 μg/ml ribostamycin (Sigma), and verified by PCR to contain both *luxS*::Kn and *rbsB*::Cm.

Autoinducer-2 production and depletion

NTHI 86-028NP and NTHI 86-028NP *rbsB*::Cm from overnight plate cultures were diluted in 20 ml of sBHI to an OD_{600} of approximately 0.05 and grown to stationary phase in sidearm flasks at 37°C with shaking at 150 rpm. Samples were taken at hourly intervals, centrifuged for 3 minutes at 13000 rpm, and supernatants were stored at −20°C until bioluminescence assays were performed. Luminescence produced by *V. harveyi* BB170 (Bassler *et al.*, 1994) following 3 h incubation with supernatant samples was determined in a Turner Designs TD-20/20 luminometer for 10 s. Data are reported as relative light units [counts per 10 s].

For AI-2 uptake studies, sBHI was supplemented with 0.2 μM (S)-4,5-Dihydroxy-2,3-pentanedione (DPD, Omm Scientific) when indicated, inoculated with ~10^8 cfu of NTHI (OD_{600} ~0.15), and incubated at 37°C and 150 rpm. Samples were taken at hourly intervals, centrifuged, and stored at −20°C as above. This concentration of DPD was chosen as it

elicits approximately equivalent luminescence from *V. harveyi* as NTHI 86-028NP late exponential phase culture supernatant (OD_{600} of approximately 0.750). For inhibition studies, NTHI 86-028NP *luxS*::Kn cultures were supplemented with ribose (Sigma), xylose (Sigma), or sucrose (Sigma) to a final concentration of 0.1, 1.0, or 10 mM as indicated and samples were taken at mid-logarithmic phase of growth (OD_{600} of ~0.85).

Real time RT-PCR

NTHI 86-028NP and NTHI 86-028NP *luxS*::Kn were grown in sBHI to stationary phase, and 0.5 ml samples were taken at the indicated optical densities for isolation of RNA as per RNeasy Mini kit instructions (Qiagen). On-column DNase treatment of samples was performed using the RNase-Free DNase set (Qiagen). RNA concentration and purity were determined using a NanoDrop ND-1000 spectrophotometer (version 3.1.2). RT-PCR master mixes were prepared using the TaqMan One-Step RT-PCR Master Mix Reagents kit (Applied Biosystems). A complete list of primers and probes is provided in Table 3 (all primers were purchased from Eurofins, and Fam/Tamra probes were purchased from Sigma). Each RT-PCR reaction was conducted in duplicate using 100 ng total RNA in a final volume of 25 μl per well. Thermocycling conditions in an ABI Prism 7000 Sequence Detection System (Applied Biosystems) were as follows: 1 cycle of 48°C for 30 minutes, 1 cycle of 95°C for 10 minutes, and 40 cycles of 95°C for 15 seconds and 60°C for 1 minute. Transcript levels were determined for *luxS*, *rbsB*, and *gyrA* using the 7000 System SDS Software (version 1.2.3f2). For each analysis, control experiments lacking reverse transcriptase treatment were performed and showed no detectable product.s

Continuous flow system

NTHI biofilms were established in a continuous-flow system as previously described (Hong *et al.*, 2007b). NTHI 86-028NP, NTHI 86-028NP *luxS*::Kn, and NTHI 86-028NP *rbsB*::Cm were diluted to ~10^8 cfu/ml in sBHI broth, injected into the port of a commercial microscopy flow-cell (Stovall), and incubated for 3 h at 37°C without medium flow to permit bacterial surface attachment. Continuous flow of sBHI media was initiated at a rate of ~60 ml per hour and maintained for 24 h.

Stationary biofilm system

NTHI stationary biofilms were established in Lab-TekII two-chamber no. 1.5 German coverglass slides (Nunc). NTHI 86-028NP, NTHI 86-028NP *luxS*::Kn, NTHI 86-028NP *rbsB*::Cm, and NTHI 86-028NP *rbsB*::Cm *IRB::rbsB* were diluted to ~10^8 cfu/ml in sBHI broth (or sBHI supplemented with 0.2 μM DPD as indicated). Chambers of the coverglass slides were inoculated with 2 ml of the bacterial suspension, and biofilms were established at 37°C and 5% CO_2 for 12 hours.

Confocal Laser Scanning Microscopy (CLSM)

Biofilm samples were washed once with PBS and stained with a LIVE/DEAD *Bac*Light viability kit (InVitrogen). Z-series images of biofilms were collected using either a Zeiss LSM510 CLSM microscope or a Nikon Eclipse C1 CLSM microscope. Between five and eight image stacks, each representing a different field of view, were compiled for each strain. The Z-series images were visualized using the Nikon Elements software and exported into MATLAB (version 5.1) for COMSTAT analysis as previously described (Heydorn *et al.*, 2002).

Whole-bacteria ELISA

ELISAs were performed on intact bacterial cells as described previously (Jones *et al.*, 2002, Armbruster *et al.*, 2009). Bacteria were diluted in distilled H_2O to an OD_{600} of 0.150 (~10^8

cfu/ml), and 0.1 ml was dispensed into each well of a MaxiSorp-coated 96-well microtiter plate (Nunc) and dried overnight uncovered at 37°C for 24 h. Plates were washed once and blocked for 30 min in TSBB buffer (10 mM Tris, 0.5 M NaCl, 0.5% Tween, pH = 8.0). Wells were incubated with 0.1 ml anti-phosphorylcholine monoclonal antibody HAS (Statens Serum Institut) overnight at room temperature, washed once, and incubated for 1 h in the dark with goat-anti-mouse IgM-horseradish peroxidase (HRP) conjugate. Wells were then washed once and incubated in the dark for approximately 20 min with 0.1 ml of TMB substrate reagent (OptEIA, Becton-Dickinson). The reaction was stopped with 0.05 ml of 2 N H_2SO_4, and OD_{450} measured using a plate reader (Labsystems Multiskan Plus).

Assessment of phase-variable genes

Determination of ON/OFF state of phase-variable genes was performed as previously described (Erwin *et al.*, 2006, Armbruster *et al.*, 2009). Individual colonies of each NTHI strain were harvested from plate cultures suspended in 0.1 ml of 10% suspension of Chelex (BioRad). Genomic DNA was prepared by vortexing suspensions for 15 sec, boiling for 10 min, chilling on ice for 2 min, and centrifugation at 8000 *x g* for 2 min. Supernatants (0.05 ml) were transferred to fresh tubes for PCR amplification and sizing by means of GeneMapper (Applied Biosystems, Inc., Foster City, CA) analysis at the DNA Sequencing Facility of the WFUHS Biomolecular Resource Laboratory as previously described (Armbruster et al., 2009). Numbers of repeats for each region were estimated based on fragment size, and used in accordance with the previously defined genomic sequence of each region to define “on” or “off” status of each phase-variable region.

Chinchilla infection studies

Bacterial persistence and biofilm formation in the middle ear cavity were assessed as described previously (Hong *et al.*, 2007a, Hong *et al.*, 2007b, Armbruster et al., 2009). Chinchillas were purchased from Rauscher’s chinchilla ranch (Larue, OH) and allowed to acclimate to the vivarium for >7 d prior to infection. No animals showed visible signs of illness prior to infection. The animals were anesthetized with isofluorane and infected via transbullar injection with ~10^3 CFU of NTHI 86-028NP, NTHI 86-028NP *luxS*::Kn, or NTHI 86-028NP *rbsB*::Cm. All inocula were confirmed by plate-counts. The degree of inflammation was assessed at 48 h intervals by digital otoscopic examination using a qualitative scoring system of 1 to 4, with 4 being the most severe (Hong et al., 2007a). Animals were euthanized at 7, 14, 21, and 28 days post-infection and bullae were aseptically opened. Fluids within the middle ear were recovered and middle ear lavage was performed using 1.0 ml sterile PBS. Both bullae were then excised and homogenized in 10 ml sterile PBS (Hong et al., 2007a). Total cfu/ear were determined by combining bacterial counts obtained for homogenized bullae and middle-ear effusion fluid with lavage.

Statistics

Significance was determined by nonparametric *t* test, unpaired *t* test, or two-way ANOVA with post-hoc tests of significance as indicated. All *P* values are two-tailed at a 95% confidence interval. Analyses were performed using GraphPad Prism, version 5 (GraphPad Software, San Diego, CA).

Acknowledgments

The authors acknowledge excellent assistance by Gayle Foster, Jim Turner, the WFU sequencing facility, and helpful comments and critiques from Dr. Steven Mizel and Dr. Marlena Westcott. This work was supported by grants from NIH/NIDCD (DC007444 and DC10051) awarded to W. E. Swords. Chelsie E. Armbruster and Kristin E.D. Weimer were supported by an NIH training grant (T32 AI07401).

References

Anderson GG, O'Toole GA. Innate and induced resistance mechanisms of bacterial biofilms. Curr Top Microbiol Immunol. 2008; 322:85–105. [PubMed: 18453273]

Armbruster CE, Hong W, Pang B, Dew KE, Juneau RA, Byrd MS, Love CF, Kock ND, Swords WE. LuxS promotes biofilmmaturation and persistence of nontypeable *Haemophilus influenzae* in vivo via modulation of lipooligosaccharides on the bacterial surface. Infect Immun. 2009; 77:4081–4091. [PubMed: 19564381]

Armbruster CE, Hong W, Pang B, Weimer KED, Juneau RA, Turner J, Swords WE. Indirect Pathogenicity of *Haemophilus influenzae* and *Moraxella catarrhalis* in Polymicrobial Otitis Media Occurs via Interspecies Quorum Signaling. mBio. 2010; 1(3):e00102-00110–e00102-00119. [PubMed: 20802829]

Armbruster CE, Swords WE. Interspecies bacterial communication as a target for therapy in otitis media. Expert Rev Anti Infect Ther. 2010; 8:1067–1070. [PubMed: 20954869]

Bakaletz LO. Bacterial biofilms in otitis media: evidence and relevance. Pediatr Infect Dis J. 2007; 26:S17–19. [PubMed: 18049376]

Bakaletz LO, Tallan BM, Hoepf T, DeMaria TF, Birck HG, Lim DJ. Frequency of fimbriation of nontypable *Haemophilus influenzae* and its ability to adhere to chinchilla and human respiratory epithelium. Infect Immun. 1988; 56:331–335. [PubMed: 2892792]

Bassler BL, Wright M, Silverman MR. Multiple signalling systems controlling expression of luminescence in *Vibrio harveyi*: sequence and function of genes encoding a second sensory pathway. Mol Microbiol. 1994; 13:273–286. [PubMed: 7984107]

Costerton JW, Stewart PS, Greenberg EP. Bacterial biofilms: a common cause of persistent infections. Science. 1999; 284:1318–1322. [PubMed: 10334980]

Costerton W, Veeh R, Shirtliff M, Pasmore M, Post C, Ehrlich G. The application of biofilm science to the study and control of chronic bacterial infections. J Clin Invest. 2003; 112:1466–1477. [PubMed: 14617746]

Davies DG, Parsek MR, Pearson JP, Iglewski BH, Costerton JW, Greenberg EP. The Involvement of Cell-to-Cell Signals in the Development of a Bacterial Biofilm. Science. 1998; 280:295–298. [PubMed: 9535661]

Ehrlich GD, Veeh R, Wang X, Costerton JW, Hayes JD, Hu FZ, Daigle BJ, Ehrlich MD, Post JC. Mucosal biofilm formation on middle-ear mucosa in the chinchilla model of otitis media. JAMA. 2002; 287:1710–1715. [PubMed: 11926896]

Erwin AL, Allen S, Ho DK, Bonthuis PJ, Jarisch J, Nelson KL, Tsao DL, Unrath WC, Watson ME Jr, Gibson BW, Apicella MA, Smith AL. Role of lgtC in resistance of nontypeable *Haemophilus influenzae* strain R2866 to human serum. Infect Immun. 2006; 74:6226–6235. [PubMed: 16966407]

Erwin AL, Smith AL. Nontypeable *Haemophilus influenzae*: understanding virulence and commensal behavior. Trends Microbiol. 2007; 15:355–362. [PubMed: 17600718]

Faden H, Waz MJ, Bernstein JM, Brodsky L, Stanievich J, Ogra PL. Nasopharyngeal flora in the first three years of life in normal and otitis-prone children. Ann Otol Rhinol Laryngol. 1991; 100:612–615. [PubMed: 1908199]

Finkelstein JA, Davis RL, Dowell SF, Metlay JP, Soumerai SB, Rifas-Shiman SL, Higham M, Miller Z, Miroshnik I, Pedan A, Platt R. Reducing Antibiotic Use in Children: A Randomized Trial in 12 Practices. Pediatrics. 2001; 108:1–7. [PubMed: 11433046]

Ghannoum, MA.; O'Toole, GA. Microbial biofilms. ASM Press; Washington, D.C.: 2004. p. xiiip. 426[410] p. of plates

Hall-Stoodley L, Hu FZ, Gieseke A, Nistico L, Nguyen D, Hayes JD, Forbes M, Greenberg DP, Dice B, Burrows A, Wackym P, Stoodley P, Post JC, Ehrlich GD, Kerschner JE. Direct detection of bacterial biofilms on the middle ear mucosa of children with chronic otitis media. JAMA. 2006; 296:202–211. [PubMed: 16835426]

Hardie KR, Heurlier K. Establishing bacterial communities by 'word of mouth': LuxS and autoinducer 2 in biofilm development. Nat Rev Microbiol. 2008; 6:635–643. [PubMed: 18536728]

Harrison A, Dyer DW, Gillaspy A, Ray WC, Mungur R, Carson MB, Zhong H, Gipson J, Gipson M, Johnson LS, Lewis L, Bakaletz LO, Munson RS Jr. Genomic sequence of an otitis media isolate of nontypeable *Haemophilus influenzae*: comparative study with *H. influenzae* serotype d, strainKW20. J Bacteriol. 2005; 187:4627–4636. [PubMed: 15968074]

Henke JM, Bassler BL. Three parallel quorum-sensing systems regulate gene expression in *Vibrio harveyi*. J Bacteriol. 2004; 186:6902–6914. [PubMed: 15466044]

Heydorn A, Ersboll B, Kato J, Hentzer M, Parsek MR, Tolker-Nielsen T, Givskov M, Molin S. Statistical analysis of *Pseudomonas aeruginosa* biofilm development: impact of mutations in genes involved in twitching motility, cell-to-cell signaling, and stationary-phase sigma factor expression. Appl Environ Microbiol. 2002; 68:2008–2017. [PubMed: 11916724]

Hoa M, Tomovic S, Nistico L, Hall-Stoodley L, Stoodley P, Sachdeva L, Berk R, Coticchia JM. Identification of adenoid biofilms with middle ear pathogens in otitis-prone children utilizing SEM and FISH. Int J Pediatr Otorhinolaryngol. 2009; 73:1242–1248. [PubMed: 19525016]

Hong W, Mason K, Jurcisek JA, Novotny LA, Bakaletz LO, Swords WE. Phosphorylcholine decreases early inflammation and promotes the establishment of stable biofilm communities of nontypeable *Haemophilus influenzae* strain 86–028NP in a chinchilla model of otitis media. Infect Immun. 2007a; 75:958–965. [PubMed: 17130253]

Hong W, Pang B, West-Barnette S, Swords WE. Phosphorylcholine expression by nontypeable *Haemophilus influenzae* correlates with maturation of biofilm communities in vitro and in vivo. J Bacteriol. 2007b; 189:8300–8307. [PubMed: 17573475]

James D, Shao H, Lamont RJ, Demuth DR. The *Actinobacillus actinomycetemcomitans* ribose binding protein RbsB interacts with cognate and heterologous autoinducer 2 signals. Infect Immun. 2006; 74:4021–4029. [PubMed: 16790775]

Jayaraman A, Wood TK. Bacterial quorum sensing: signals, circuits, and implications for biofilms and disease. Annu Rev Biomed Eng. 2008; 10:145–167. [PubMed: 18647113]

Jones PA, Samuels NA, Phillips NJ, Munson RS, Bozue JA, Arseneau JA, Nichols WA, Zaleski A, Gibson BW, Apicella MA. *Haemophilus influenzae* type B strain A2 has multiple sialyltransferases involved in lipooligosaccharide sialylation. J Biol Chem. 2002; 277:14598–14611. [PubMed: 11842084]

Kendall MM, Rasko DA, Sperandio V. Global effects of the cell-to-cell signaling molecules autoinducer-2, autoinducer-3, and epinephrine in a *luxS* mutant of enterohemorrhagic *Escherichia coli*. Infect Immun. 2007; 75:4875–4884. [PubMed: 17635870]

Klein JO. The burden of otitis media. Vaccine. 2000; 19:S2–8. [PubMed: 11163456]

Li J, Attila C, Wang L, Wood TK, Valdes JJ, Bentley WE. Quorum sensing in *Escherichia coli* is signaled by AI-2/LsrR: effects on small RNA and biofilm architecture. J Bacteriol. 2007; 189:6011–6020. [PubMed: 17557827]

Mandel EM, Doyle WJ, Winther B, Alper CM. The incidence, prevalence and burden of OM in unselected children aged 1–8 years followed by weekly otoscopy through the “common cold” season. Int J Pediatr Otorhinolaryngol. 2008; 72:491–499. [PubMed: 18272237]

Michiko E, Taga JLSBLB. The LuxS-dependent autoinducer AI-2 controls the expression of an ABC transporter that functions in AI-2 uptake in *Salmonella typhimurium*. Mol Microbiol. 2001; 42:777–793. [PubMed: 11722742]

Miller MB, Bassler BL. Quorum sensing in bacteria. Annu Rev Microbiol. 2001; 55:165–199. [PubMed: 11544353]

Miller ST, Xavier KB, Campagna SR, Taga ME, Semmelhack MF, Bassler BL, Hughson FM. *Salmonella typhimurium* recognizes a chemically distinct form of the bacterial quorum-sensing signal AI-2. Mol Cell. 2004; 15:677–687. [PubMed: 15350213]

Nistico L, Kreft R, Gieseke A, Coticchia JM, Burrows A, Khampang P, Liu Y, Kerschner JE, Post JC, Lonergan S, Sampath R, Hu FZ, Ehrlich GD, Stoodley P, Hall-Stoodley L. An Adenoid Reservoir for Pathogenic Biofilm Bacteria. J Clin Microbiol. 2011 JCM.00756–00710.

Pereira CS, McAuley JR, Taga ME, Xavier KB, Miller ST. *Sinorhizobium meliloti*, a bacterium lacking the autoinducer-2 (AI-2) synthase, responds to AI-2 supplied by other bacteria. Mol Microbiol. 2008; 70:1223–1235. [PubMed: 18990189]

Pichichero ME. Recurrent and persistent otitis media. Pediatr Infect Dis J. 2000; 19:911–916. [PubMed: 11001126]

Post JC. Direct evidence of bacterial biofilms in otitis media. Laryngoscope. 2001; 111:2083–2094. [PubMed: 11802002]

Post JC, Hiller NL, Nistico L, Stoodley P, Ehrlich GD. The role of biofilms in otolaryngologic infections: update 2007. Curr Opin Otolaryngol Head Neck Surg. 2007; 15:347–351. [PubMed: 17823552]

Rezzonico F, Duffy B. Lack of genomic evidence of AI-2 receptors suggests a non-quorum sensing role for *luxS* in most bacteria. BMC Microbiol. 2008; 8:154. [PubMed: 18803868]

Shao H, James D, Lamont RJ, Demuth DR. Differential interaction of *Aggregatibacter (Actinobacillus) actinomycetemcomitans* LsrB and RbsB proteins with autoinducer 2. J Bacteriol. 2007a; 189:5559–5565. [PubMed: 17526716]

Shao H, Lamont RJ, Demuth DR. Autoinducer 2 Is Required for Biofilm Growth of *Aggregatibacter (Actinobacillus) actinomycetemcomitans*. Infect Immun. 2007b; 75:4211–4218. [PubMed: 17591788]

Stewart PS. Mechanisms of antibiotic resistance in bacterial biofilms. Int J Med Microbiol. 2002; 292:107–113. [PubMed: 12195733]

Sztajer H, Lemme A, Vilchez R, Schulz S, Geffers R, Yip CY, Levesque CM, Cvitkovitch DG, Wagner-Döbler I. Autoinducer-2-regulated genes in *Streptococcus mutans* UA159 and global metabolic effect of the *luxS* mutation. J Bacteriol. 2008 Epub ahead of print.

Taga ME, Miller ST, Bassler BL. Lsr-mediated transport and processing of AI-2 in *Salmonella typhimurium*. Mol Microbiol. 2003; 50:1411–1427. [PubMed: 14622426]

Taga ME, Semmelhack JL, Bassler BL. The LuxS-dependent autoinducer AI-2 controls the expression of an ABC transporter that functions in AI-2 uptake in *Salmonella typhimurium*. Molecular Microbiology. 2001; 42:777–793. [PubMed: 11722742]

Verhaegh SJ, Snippe ML, Levy F, Verbrugh HA, Jaddoe VW, Hofman A, Moll HA, van Belkum A, Hays JP. Colonization of healthy children by Moraxella catarrhalis is characterized by genotype heterogeneity, virulence gene diversity and co-colonization with Haemophilus influenzae. Microbiology. 157:169–178. [PubMed: 20847012]

Wang L, Li J, March JC, Valdes JJ, Bentley WE. *luxS*-dependent gene regulation in *Escherichia coli* K-12 revealed by genomic expression profiling. J Bacteriol. 2005; 187:8350–8360. [PubMed: 16321939]

Waters CM, Bassler BL. Quorum sensing: cell-to-cell communication in bacteria. Annu Rev Cell Dev Biol. 2005; 21:319–346. [PubMed: 16212498]

Weiser JN. The generation of diversity by *Haemophilus influenzae*. Trends Microbiol. 2000; 8:433–435. [PubMed: 11044669]

West-Barnette S, Rockel A, Swords WE. Biofilm growth increases phosphorylcholine content and decreases potency of nontypeable *Haemophilus influenzae* endotoxins. Infect Immun. 2006; 74:1828–1836. [PubMed: 16495557]

Whitby PW, Morton DJ, Stull TL. Construction of antibiotic resistance cassettes with multiple paired restriction sites for insertional mutagenesis of *Haemophilus influenzae*. FEMS Microbiol Lett. 1998; 158:57–60. [PubMed: 9453156]

Winzer K, Hardie KR, Burgess N, Doherty N, Kirke D, Holden MT, Linforth R, Cornell KA, Taylor AJ, Hill PJ, Williams P. LuxS: its role in central metabolism and the *in vitro* synthesis of 4-hydroxy-5-methyl-3(2H)-furanone. Microbiology. 2002; 148:909–922. [PubMed: 11932438]

Winzer K, Hardie KR, Williams P. LuxS and autoinducer-2: Their contribution to quorum sensing and metabolism in bacteria. Adv Appl Microbiol. 2003; 53:291–396. [PubMed: 14696323]

Xavier KB, Bassler BL. Regulation of uptake and processing of the quorum-sensing autoinducer AI-2 in *Escherichia coli*. J Bacteriol. 2005; 187:238–248. [PubMed: 15601708]

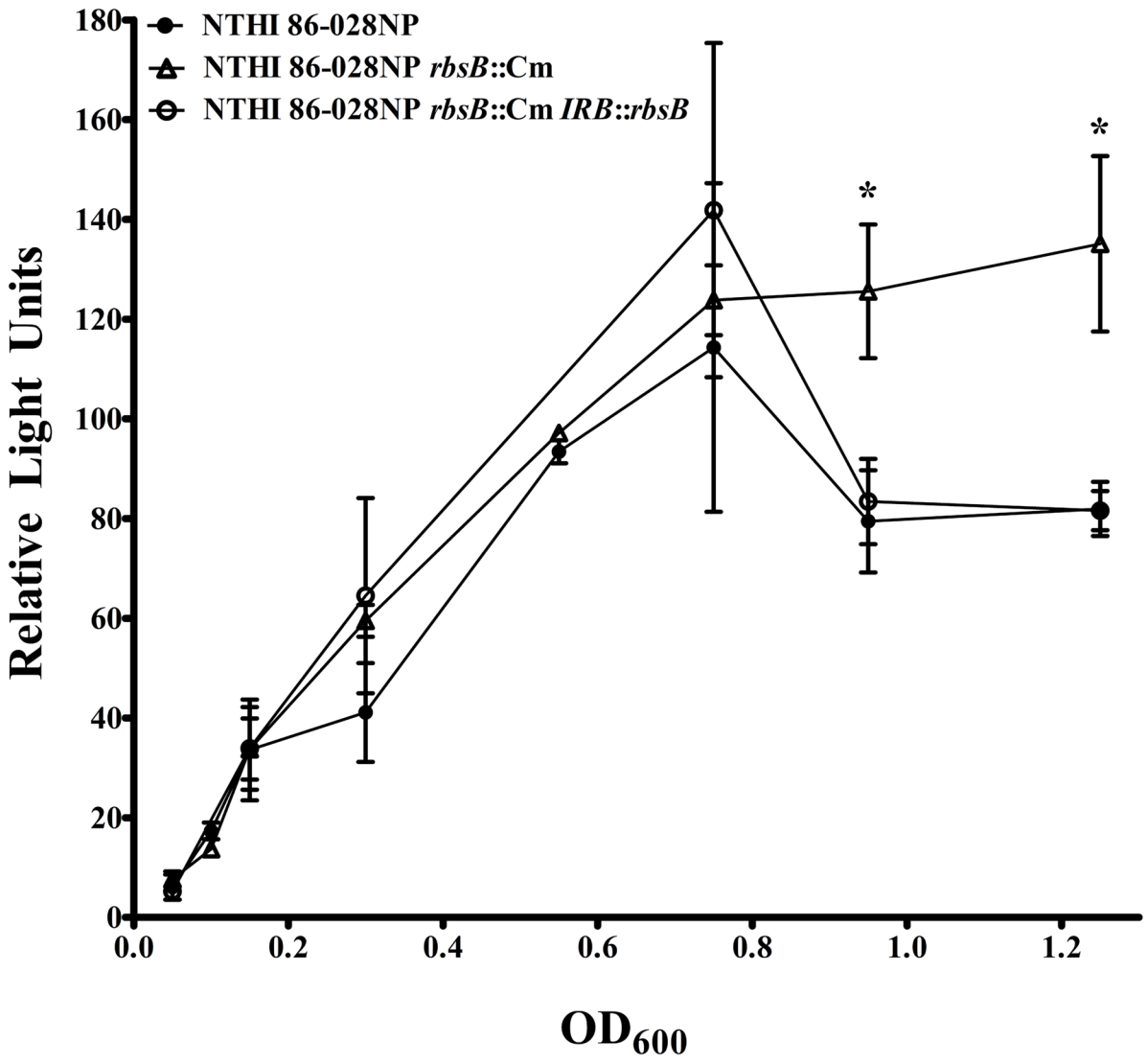

Figure 1. AI-2 accumulates in late-exponential phase cultures of NTHI 86-028NP *rbsB*::Cm

NTHI 86-028NP, NTHI 86-028NP *rbsB*::Cm, and the complemented strain NTHI 86-028NP *rbsB*::Cm *IRB*::Sp were cultured in sBHI to stationary phase and supernatant samples were removed and stored at −20°C. Determination of AI-2 production in thawed supernatants was performed using the *Vibrio harveyi* bioluminescence assay. Significance was determined by a two-way ANOVA with a post-hoc test. **P*<0.05. Error bars indicate mean and standard deviation for three independent experiments and duplicate samples for bioluminescence.

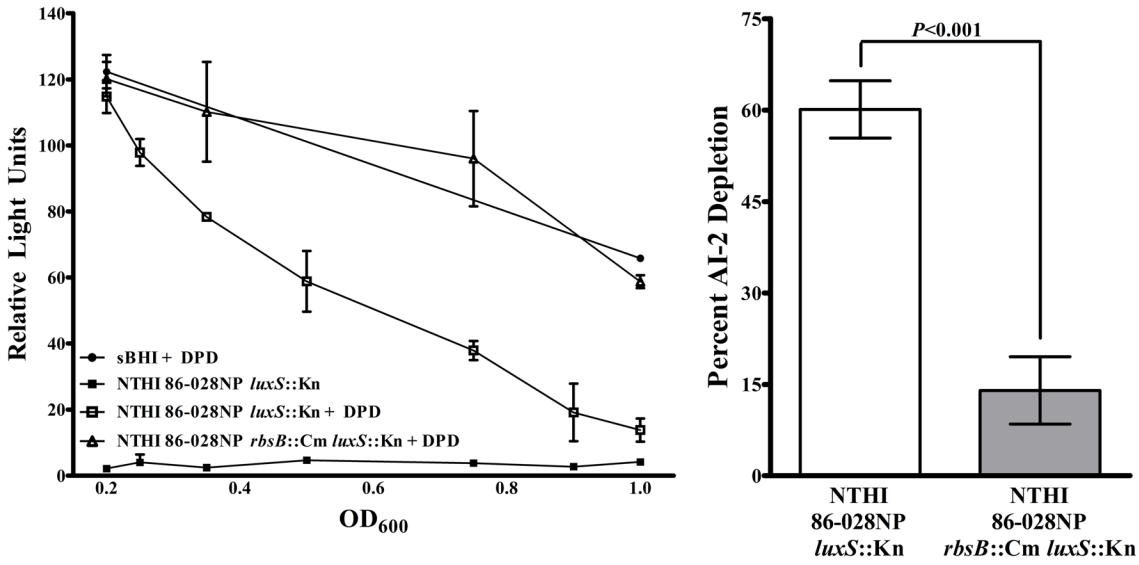

Figure 2. Mutation of *rbsB* limits AI-2 depletion

NTHI 86-028NP *luxS*::Kn and NTHI 86-028NP *rbsB*::Cm *luxS*::Kn were cultured in sBHI media alone or sBHI supplemented with 0.2 μM of the chemically synthesized AI-2 precursor (S)-4,5-Dihydroxy-2,3-pentanedione (DPD) and samples were taken to assess depletion of DPD by *V. harveyi* bioluminescence. An uninoculated control sample of sBHI supplemented with DPD was included as a negative control for depletion. (A) A representative graph showing kinetics of AI-2 depletion by NTHI 86-028NP *luxS*::Kn and NTHI 86-028NP *rbsB*::Cm *luxS*::Kn. Error bars indicate mean and standard deviation for duplicate samples. (B) Combined results of five independent experiments with duplicate samples showing the percent of AI-2 depleted by NTHI 86-028NP *luxS*::Kn versus NTHI 86-028NP *rbsB*::Cm *luxS*::Kn for culture supernatants taken at an OD_{600} of ~0.85, normalized to uninoculated control samples. Error bars indicate mean and standard deviation.

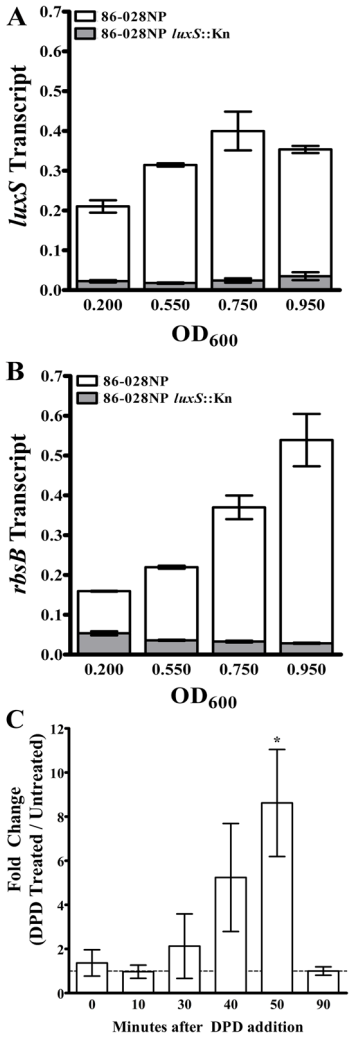

Figure 3. AI-2 increases transcription of *luxS* and *rbsB*

NTHI 86-028NP and NTHI 86-028NP *luxS*::Kn were cultured in sBHI media to stationary phase. Samples were taken during lag phase (OD_{600} 0.200), exponential phase (OD_{600} 0.500), late-exponential phase (OD_{600} 0.750), and early stationary phase (OD_{600} 0.950) for isolation of RNA and real time RT-PCR analysis of *luxS* (A) and *rbsB* (B) transcript levels. Values represent the ratio of *luxS* or *rbsB* to *gyrA* transcript. Error bars indicate mean and standard deviation for duplicate samples. (C) NTHI 86-028NP *luxS*::Kn was cultured in sBHI to an OD_{600} of ~0.650 and supplemented with either 0.2 μM DPD or sterile water. Samples were taken prior to the addition of DPD or water and at 10, 30, 40, 50, and 90 minutes afterwards for RNA isolation and real time RT-PCR analysis of *rbsB* transcript levels. Values represent the fold increase in *rbsB* transcript (normalized to *gyrA*) for the DPD treated samples compared to untreated samples. Error bars indicate mean and standard deviation for duplicate sampling from two independent experiments.

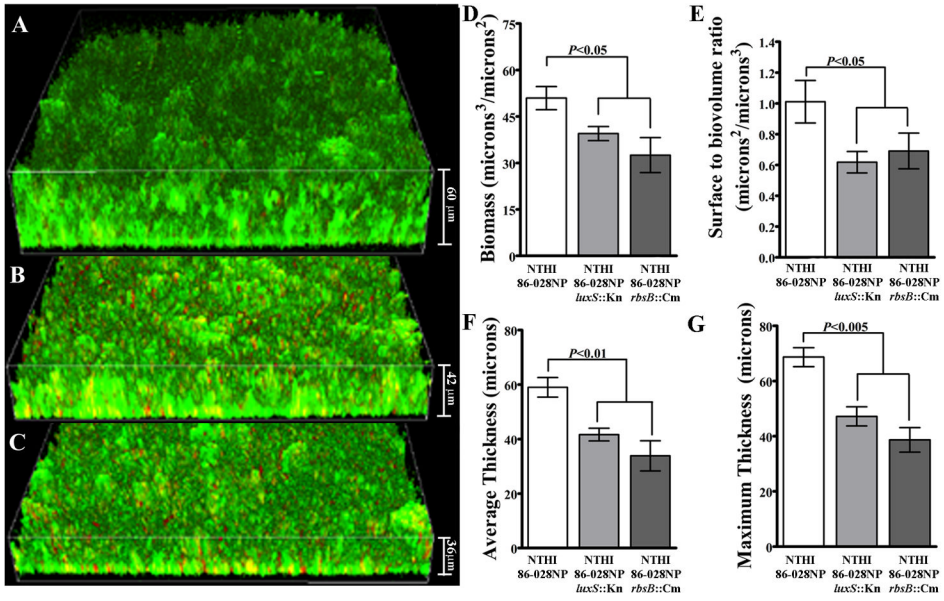

Figure 4. Mutation of *rbsB* results in a similar biofilm defect as mutation of *luxS*

Biofilms formed by NTHI 86-028NP, NTHI 86-028NP *luxS*::Kn, and NTHI 86-028NP *rbsB*::Cm under continuous flow conditions were visualized with a live/dead stain by CLSM. Z-series images were used to create representative volume views of biofilms formed by NTHI 86-028NP (A), NTHI 86-028NP *luxS*::Kn (B), and NTHI 86-028NP *rbsB*::Cm (C). Z-series images were also exported to COMSTAT to obtain biofilm measurements, including total biomass (D), surface to biovolume ratio (E), average biofilm thickness (F), and maximum biofilm thickness (G). Statistical significance determined by unpaired *t* test, error bars indicate standard error of the mean (n=8).

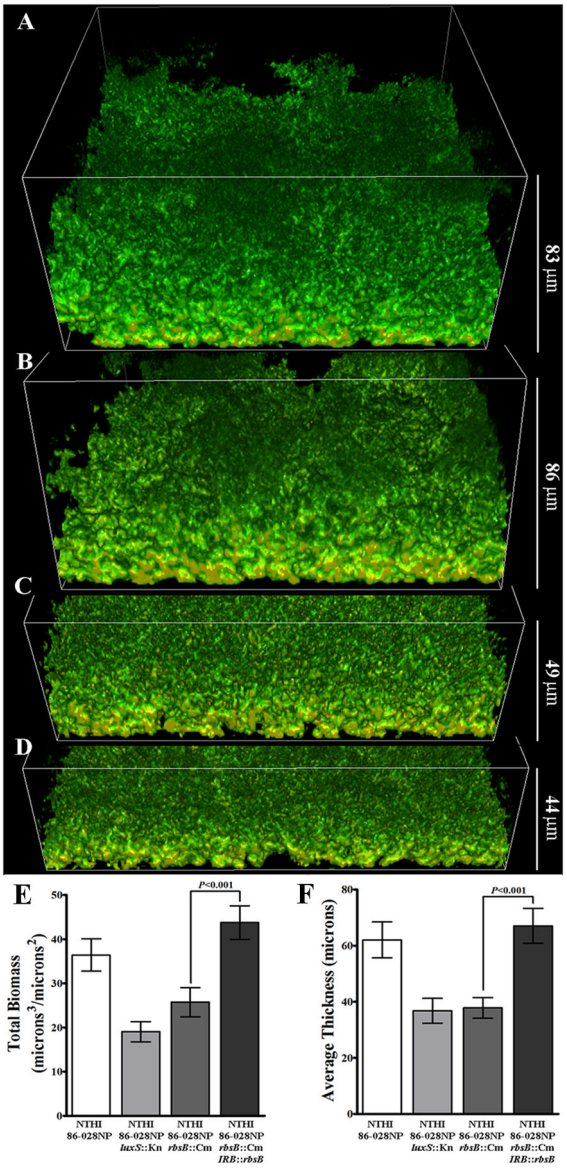

Figure 5. Genetic complementation fully restores biofilm formation by NTHI 86-028NP *rbsB*::Cm

NTHI 86-028NP, NTHI 86-028NP *luxS*::Kn, NTHI 86-028NP *rbsB*::Cm, and the complemented strain NTHI 86-028NP *rbsB*::Cm *IRB::rbsB* were cultured in sBHI media and allowed to establish stationary biofilms for 12 h. Biofilms were visualized by live/dead staining and CLSM. Vertical z-series images were used to create representative volume views of biofilms formed by NTHI 86-028NP (A), NTHI 86-028NP *rbsB*::Cm *IRB::rbsB* (B), NTHI 86-028NP *rbsB*::Cm (C), and NTHI 86-028NP *luxS*::Kn (D). Z-series images were also exported to COMSTAT to obtain measurements of total biofilm biomass (E) and average thickness (F). Statistical significance determined by unpaired *t* test. Error bars indicate mean and standard deviation (n=6).

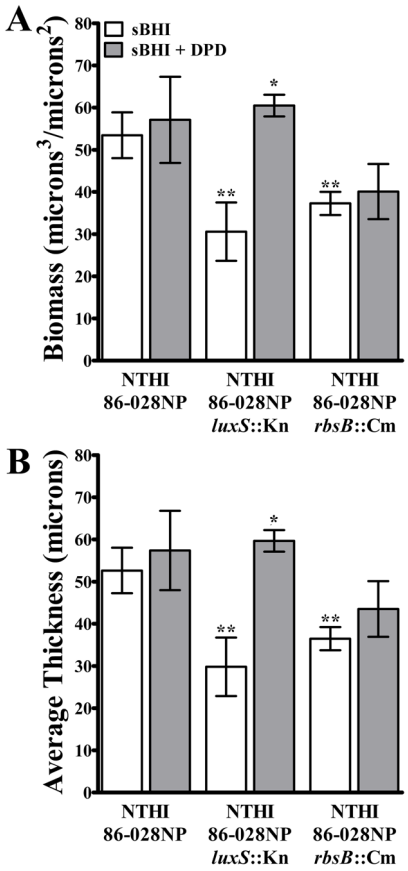

Figure 6. NTHI 86-028NP requires *rbsB* to respond to exogenous AI-2

NTHI 86-028NP, NTHI 86-028NP *luxS*::Kn, and NTHI 86-028NP *rbsB*::Cm were cultured in sBHI media alone (white bars) or sBHI supplemented with 0.2 μM DPD (gray bars) and allowed to establish stationary biofilms for 12 h. Biofilms were visualized by live/dead staining and CLSM. Vertical z-series images were exported to COMSTAT for analysis of total biofilm biomass (A) and average thickness (B). Statistical significance determined by unpaired *t* test. ** $P<0.01$ compared to NTHI 86-028NP. * $P<0.01$ compared to NTHI 86-028NP *luxS*::Kn. Error bars indicate mean and standard deviation (n=6).

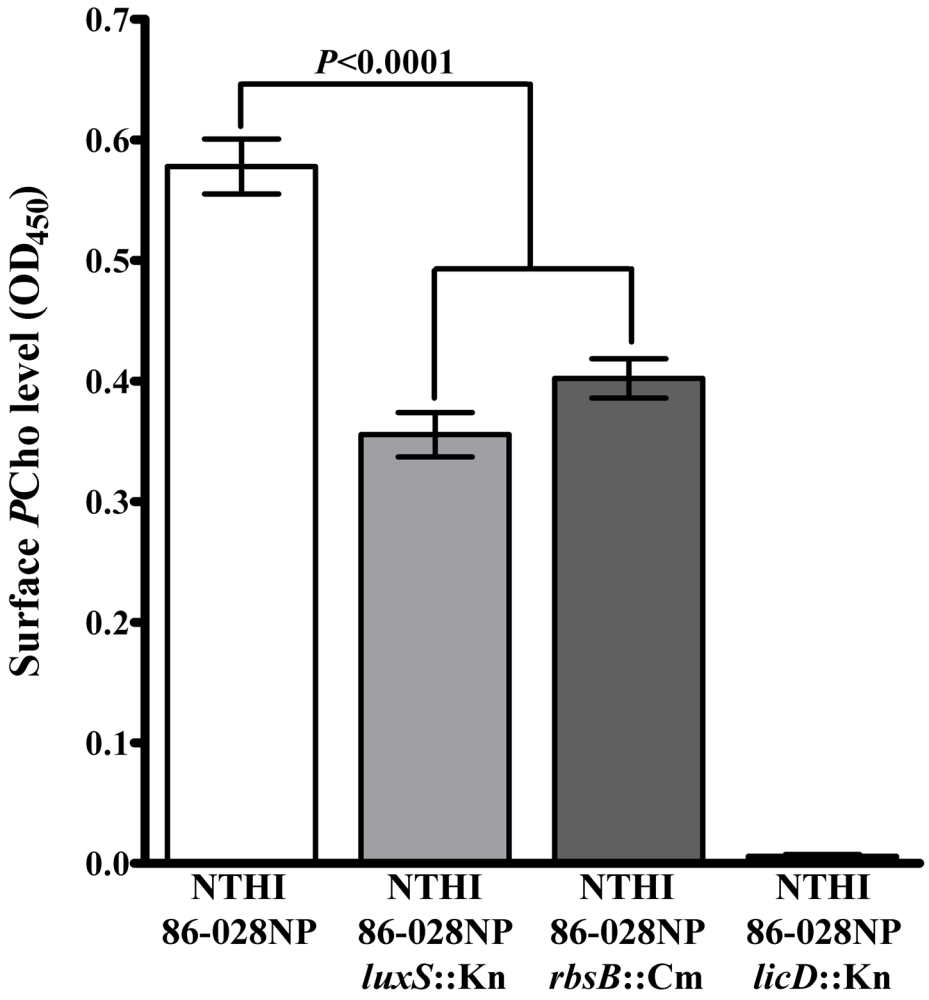

Figure 7. Mutation of *rbsB* reduces surface-accessible *P*Cho

A modified whole-bacterium ELISA was used to detect surface phosphorylcholine using an anti-*P*Cho monoclonal antibody. Significance determined by unpaired *t* test, error bars indicate standard error of the mean (n=12).

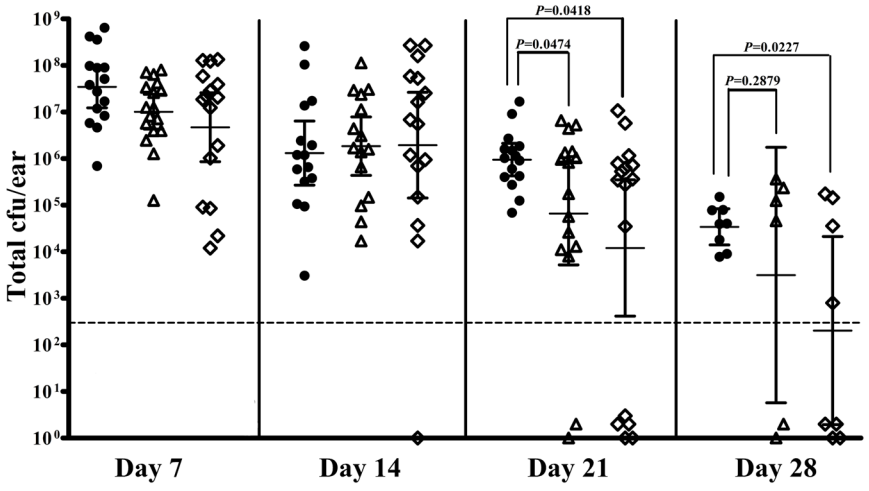

Figure 8. Mutation of *rbsB* limits bacterial persistence in vivo

Chinchillas were infected via transbullar inoculation with ~10^3 cfu of NTHI 86-028NP (filled circles), NTHI 86-028NP *luxS*::Kn (open triangles), or NTHI 86-028NP *rbsB*::Cm (open diamonds). Total bacterial load per ear was determined by serial dilution and plating of effusion fluid, middle ear lavage, and bullar homogenate at 7, 14, 21, and 28 days post-infection. Data points represent total bacterial load for individual ears, and data shown are the combined results for three independent studies (two 21-day studies and one 28-day study). Day 7: NTHI 86-028NP n=15 ears, NTHI 86-028NP *luxS*::Kn n=17 ears, NTHI 86-028NP *rbsB*::Cm n=15 ears. Day 14: NTHI 86-028NP n=15 ears, NTHI 86-028NP *luxS*::Kn n=15 ears, NTHI 86-028NP *rbsB*::Cm n=15 ears. Day 21: NTHI 86-028NP n=14 ears, NTHI 86-028NP *luxS*::Kn n=16 ears, NTHI 86-028NP *rbsB*::Cm n=16 ears. Day 28: NTHI 86-028NP n=8 ears, NTHI 86-028NP *luxS*::Kn n=6 ears, NTHI 86-028NP *rbsB*::Cm n=8 ears. The dashed line indicates limit of detection. Error bars represent the geometric mean and 95% confidence intervals. Significance determined by log transformation of the data and unpaired *t* test.

Table 1

Inhibition of DPD depletion

Treatment	Percent DPD Depletion[a]	Standard Deviation	*P* Value[b]
No Treatment	58.66	10.91	-
Ribose			
0.1 mM	42.68	7.92	0.07
1.0 mM	34.12	3.57	**0.01**
10 mM	2.28	10.02	< **0.01**
Xylose			
0.1 mM	60.46	10.72	0.98
1.0 mM	66.65	2.33	0.07
10 mM	0.93	16.83	< **0.01**
Sucrose			
0.1 mM	60.50	1.13	0.19
1.0 mM	61.20	10.89	0.17
10 mM	58.10	2.26	0.10

[a] Percent DPD depleted from culture at an OD_{600} of approximately 0.800 compared to an uninoculated control.

[b] *P* values determined by unpaired *t* test of percent DPD depletion with the indicated treatment compared to an untreated control.

Table 2

Analysis of tetrameric repeat regions

	NTHI 86-028NP	NTHI 86-028NP *rbsB*::Cm
	Number of colonies	**Number of colonies**
oafA		
ON	8	7
OFF	24	1
lex2A		
ON	2	0
OFF	32	6
lic1A		
ON	31	8
OFF	0	0
lic2A		
ON	24	8
OFF	0	0
lic3A		
ON	24	7
OFF	0	0
lic3A2		
ON	8	8
OFF	0	0
lgtC		
ON	38	8
OFF	0	0
[a]1769		
ON	8	8
OFF	0	0
lav		
ON	0	0
OFF	8	7

[a]1769 refers to NTHI_1769, a hypothetical glycosyltransferase

Table 3

Real time PCR primers

Primer	Sequence
gyrA Forward	5′-GCATTACCTGACGTTCGAGATG-3′
gyrA Reverse	5′-CCTTCGCGATCCATTGAGAA-3′
gyrA Probe	5′-6TTTAAAACCAGTTCACCGCCGCGTAC0-3′
luxS Forward	5′-TGCGGAAGCTATACGGAACA-3′
luxS Reverse	5′-CCTATACCGCGTGCGATAACA-3′
luxS Probe	5′-6TCCTTAGAAGATGCACACGAAATTGCCAA0-3′
rbsB Forward	5′-TGATGCTCATAAATTCAATGTGCTT-3′
rbsB Reverse	5′-TTTCCGTTACATTCAAACCTTTTG-3′
rbsB Probe	5′-6CCAGTCAGCCAGCAGATTTTGATCGA0-3′